Superconducting Transition Metal Nitride Films for THz SIS Mixers

N. N. Iosad, V. V. Roddatis, S. N. Polyakov, A. V. Varlashkin, B. D. Jackson, P. N. Dmitriev, J. R. Gao, and T. M. Klapwijk

Abstract—The development of sensitive THz SIS mixers requires a low-loss superconducting strip-line material with a transition temperature above 15 K. In this paper we examine the properties of (Nb,Ti)N, NbN, and (Nb,Zr)N thin films sputtered at ambient substrate temperature on glass wafers. The best properties are observed for the (Nb,Ti)N films, sputtered from an NbTi alloy target with 30 at. % Ti. A similar picture is observed for the epitaxial films deposited on the MgO wafers. We have also examined the homogeneity of the (Nb,Ti)N films versus film thickness and in plane since this factor is clearly important for the micro-wave behavior of the strip-line. We observe that (Nb,Ti)N films deposited on silicon, sapphire, and glass wafers have much worse homogeneity compared to the films deposited on the MgO wafers.

***Index Terms*— Magnetron sputtering, SIS mixers, transition metals nitrides.**

I. Introduction

The nitrides of transition metals have been a matter of strong interest for the last 30 years among the superconducting community. The primary advantage of these materials is the simple method for thin film production like reactive magnetron sputtering at ambient substrate temperature. This enables a broad range of device applications, including RSFQ, SQUID, and THz mixers [1]-[7]. Our particular interest is motivated by the development of the Nb SIS – based mixers with tuning elements out of B1 type superconductor. For this application we need reproducible films with the lowest possible resistivity, the highest possible transition temperature (T_c), and intrinsic stress that does not cause the peeling of the film layers or photoresist. Different authors have reported a broad range of sometimes contradictory results regarding the properties of those films. These considerations lead us to the conclusion that a systematic experimental study is needed.

II. Experimental

Films of nitrides are deposited by reactive magnetron sputtering in a Nordiko-2000 sputtering system with a base pressure of $4\cdot10^{-5}$ Pa. This machine is equipped with a cryopump and a throttling valve, which together determine the process pressure, while the injection of Ar and N_2 gases is controlled by flow meters. In order to avoid the hysteretic sputtering regime, the pumping rate is fixed at a high value of 750 l/s for all experiments [8]. Alloy targets of NbTi and NbZr are used for the deposition of solid solutions of transition metals. The purity of all targets is 99.8 at. % or better. Because the process of target erosion affects film properties, we have used fresh targets for all experiments. The depth of erosion tracks is less than 10 % of the 6 mm thick targets. In order to maximize film uniformity, the substrate-target distance is set to the maximum for our sputtering system, 8 cm. All films are sputtered with 300 W dc power, resulting in a deposition rate of 80±10 nm/min. The substrates are fixed to a copper chuck with diffusion pump oil, which is maintained at 10° C to stabilize the thermodynamics of growth. Since our sputtering source is located above the substrate holder no clamping is used additionally. The amount of oil used between the substrate and the chuck is carefully monitored to avoid possible contamination of the growing film. Our SIS devices are being routinely produced in this way with excellent reproducibility. The stress in the films is evaluated by measuring the deflection of the wafer before and after film deposition with a profilometer. The stress value is calculated with the help of Stoney's equation [9], using a Young's modulus and Poisson's ratio for the glass wafers taken from [10]. T_c is evaluated from the dependence of film resistivity on temperature. The width of the transition to the superconducting state is studied by measuring the ac magnetic field susceptibility versus temperature [11]. Film resistivity is measured at 20 K, since this parameter is representative of rf-losses in a microwave strip-line and also more informative from the perspective of the concentration of the quenched-in crystal point defects. RRR value is measured as a ratio of the film resistivities at room temperature and 20 K. X-Ray diffraction (XRD) data is collected using a Rigaku D/max-Rc diffractometer equipped with a thin-film diffractometer and pole-figure goniometer. Cross-sectional samples are prepared by a standard technique - mechanical thinning down to 30 μm, followed by ion milling using a Gatan 600 Duo Ion Mill. The specimens are examined with a Philips EM430ST transmission electron microscope (TEM) operated at 200kV.

III. Comparison of Differernt Nitrides

In order to select the best material for our application we have sputtered 500 nm thick films of different compositions on glass wafers. The optimum ratio of Nb and Ti in the sputtering target is determined by comparing the maximum possible T_c of (Nb,Ti)N films sputtered from targets with different compositions. We have selected the NbTi target with 30 at. % Ti content for further studies,

Manuscript received September 17, 2000. This work was supported in part by RFBR project 00-02-16270, INTAS project 97-1712, ESA contract nr. 11653/95.

N. N. Iosad and T. M. Klapwijk are with the Delft University of Technology, Department of Applied Physics (DIMES), Lorentzweg 1, 2628 CJ Delft, The Netherlands (e-mail: iosad@dimes.tudelft.nl).

V. V. Roddatis is with the Institute of Crystallography Russian Academy of Sciences, Leninsky pr. 59, 117333 Moscow, Russia.

S. N. Polyakov is with the Institute of Nuclear Physics, Moscow State University, 119899, GSP, Moscow, Russia.

A. V. Varlashkin is with the P. N. Lebedev Physical Institute Leninsky pr. 53, 117924, Moscow, Russia.

B. D. Jackson and J .R. Gao are with the Space Research Organization of the Netherlands, PO Box 800, 9700 AV, Groningen, The Netherlands.

P. N. Dmitriev Institute of Radioelectronics Russian Academy of Sciences, Mokhovaya 11, 103907, GSP-3, Moscow, Russia

since it provides the highest possible Ti content in the deposited films without T_c degradation. Taking into account the data published in [12], which show similar properties for (Nb,Zr)N and (Nb,Ti)N thin films, we have also used a NbZr alloy target with 30 at. % Zr for the studies of (Nb,Zr)N.

The properties of NbN, (Nb,Ti)N, (Nb,Zr)N are illustrated on Fig. 1. The lower edge of the pressure range is determined by an increase in compressive stress, while the upper pressure limit is determined by an increase of film resistivity, which makes the films unacceptable for device production. Nitrogen injection is optimized to achieve the highest possible T_c for each sputtering pressure. It is found that T_c has only a moderate dependence on pressure, while film resistivity increases sharply at high pressures. This is due to the absence of a high peak in the density-of-states at the Fermi level (unlike A15 compounds) that makes the T_c of B1 superconductors insensitive to disorder defects. The intrinsic stress curves show a normal behavior, with a rapid increase in compressive stress at low pressures. The RRR is in the vicinity of unity for all the films, indicating that film resistivty is determined by crystal defects. XRD analysis reveals that all films have a B1 crystal structure with [100] texture at low sputtering pressures and [111] texture at high sputtering pressures for all materials.

One interesting point is that NbN and (Nb,Ti)N thin films show a flattening of the stress curves at high pressures with a corresponding sharp rise in film resistivty, while (Nb,Zr)N films show a monotonous increase in stress and only a moderate increase in film resistivity. This is due to the fact that the flattening of the stress curve at high pressures is caused by a transition of film structure from ZT to Z1, according to the Thornton classification [13]. Films corresponding to Z1 structural zone have voids on the grain boundaries, which strongly affect the film resistivity [14].

We have also compared the properties of (Nb,Ti)N and NbN films sputtered on MgO [100] wafers. (Nb,Zr)N films are not included in this experiment because of their low T_c. XRD analysis shows that all films deposited on MgO wafers are epitaxial and have a mosaic film stucture. Details of the XRD analysis technique for epitaxial films are published elsewhere [15]. All films characterized in Fig. 2 are 500 nm thick. Nitrogen injection is optimized to produce maximum T_c for every sputtering pressure. In general, T_c and RRR have only a moderate dependence on sputtering pressure, while film resistivity increases considerably at high pressures. We believe that the degradation in film properties at high pressures is due to the development of voids between the blocks in the mosaic structure and an increase in the quenched-in vacancy concentration. In contrast with the films sputtered on glass wafers, we observe a flattening of the curves at low pressures, which is a clear advantage from the prospective of film reproducibility.

NbN films deposited on Si wafers covered by rf-sputtered MgO (100 nm thick), show a more pronounced [100] texture and lower resistivity when compared with the NbN films sputtered on bare Si wafers under the same deposition conditions. However since we do not see a T_c improvement in NbN films by utilizing MgO under-layers we have not studied this technological approach extensively.

IV. Film Homoginiety

Because the magnetic field penetration in (Nb,Ti)N films is almost equal to the thickness of the layers ($\approx$ 300 nm) we are currently using as bottom metal layers in strip-lines for THz mixers, film homogeneity is a very important issue. Fig. 3 illustrates the the T_c and film resistivity for different (Nb,Ti)N film thickness and wafer materials. All films are deposited under 6 mTorr sputtering pressure, since these conditions provide the lowest film resistivty

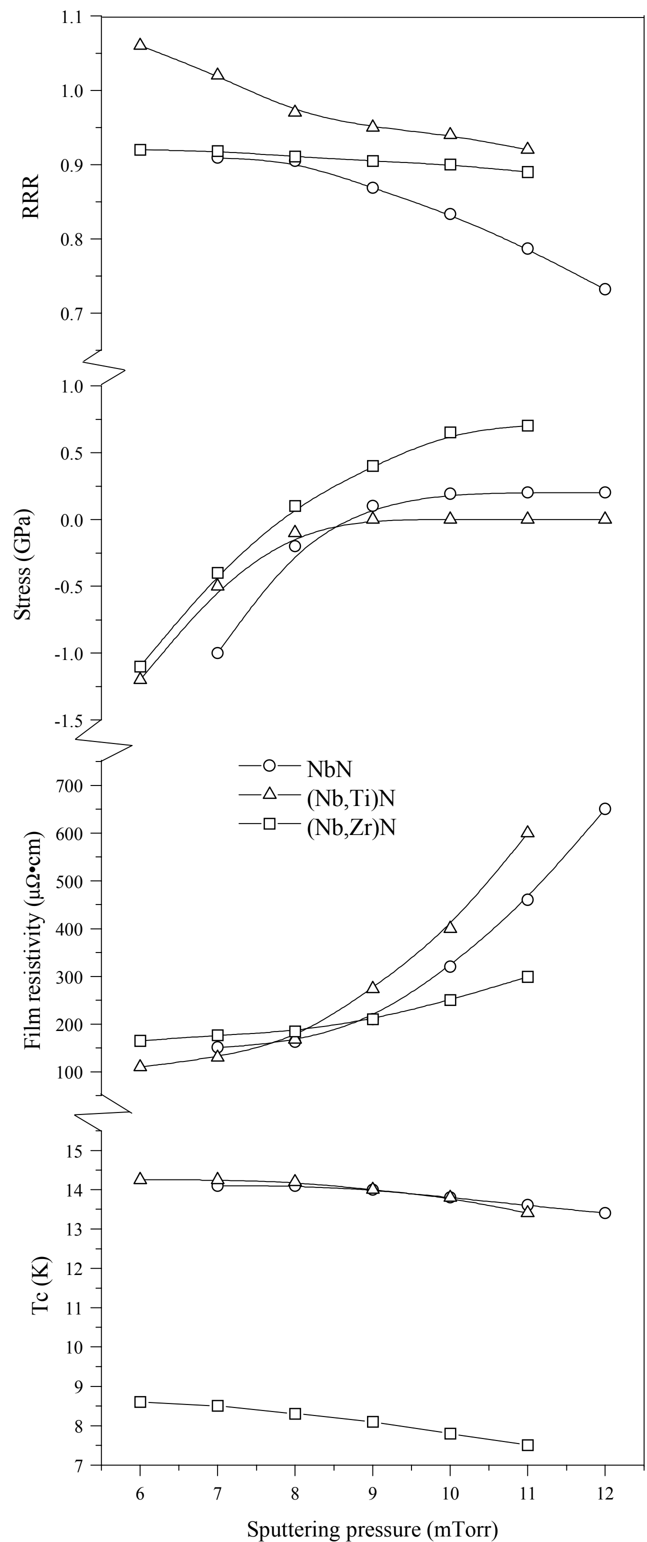

Fig. 1 RRR, intrinsic stress, film resitivity, and transition temperature of (Nb,Ti)N, (Nb,Zr)N, NbN films deposited on glass wafers at ambient substrate temperature.

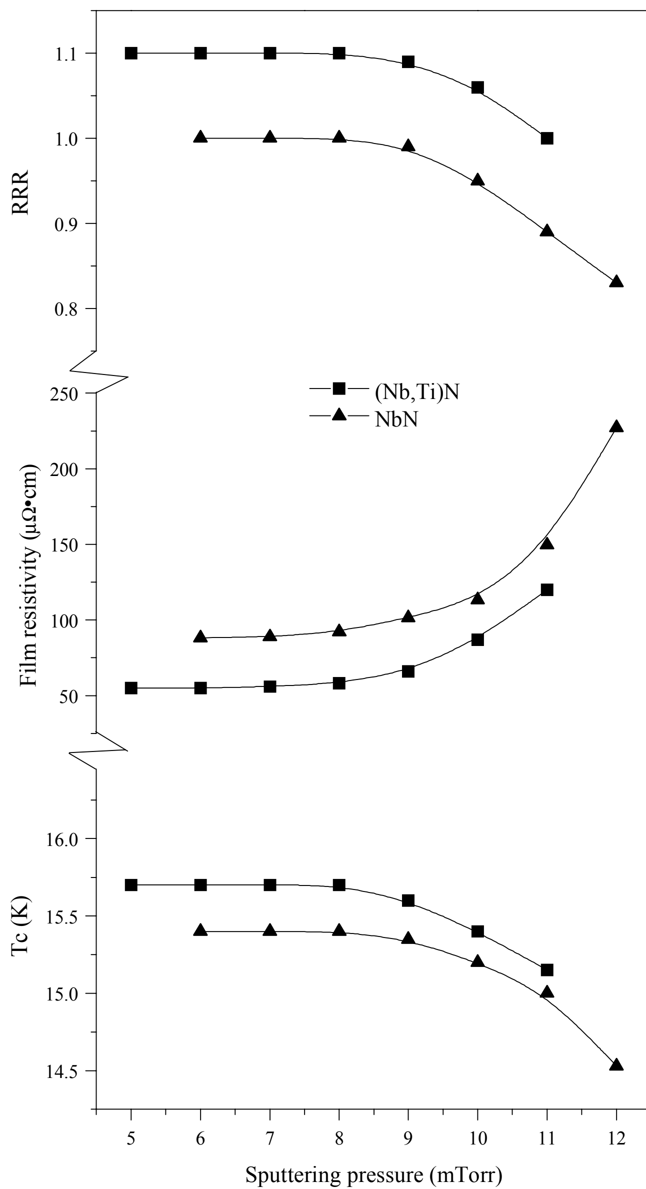

Fig. 2 RRR, film resitivity, and transition temperature of the (Nb,Ti)N, NbN films deposited on MgO wafers.

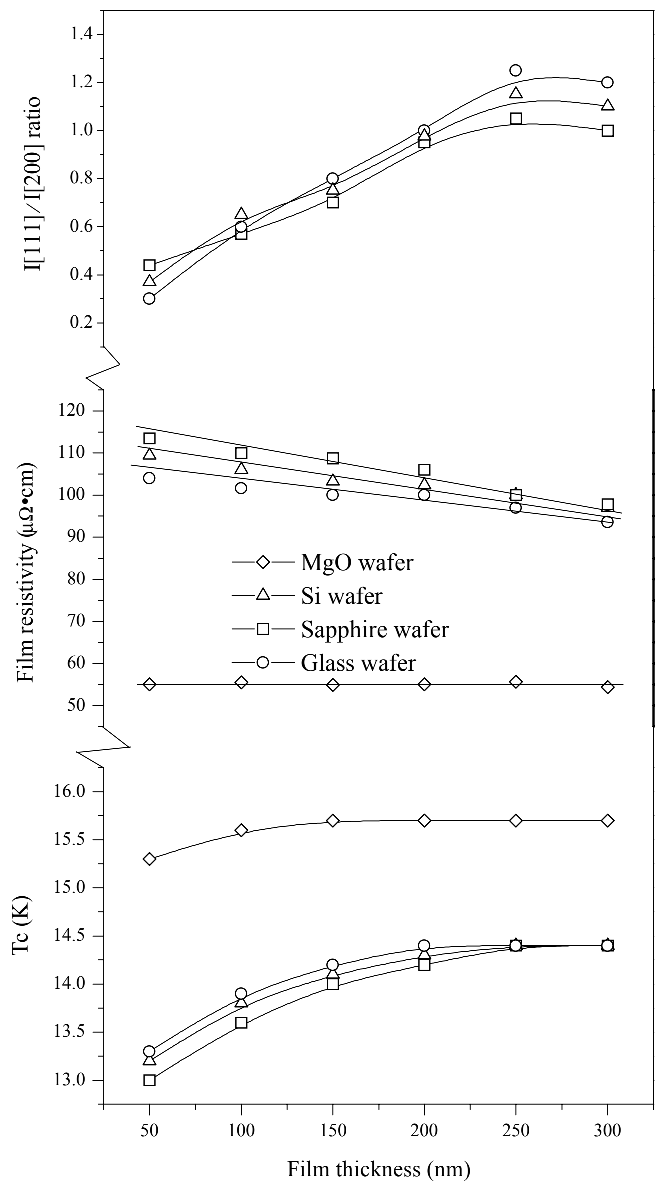

Fig. 3 Ratio of [111]and [200] XRD peak intensity, film resitivity and transition temperature of the (Nb,Ti)N films, deposited on MgO, sapphire, Si, and glass wafers.

and the highest T_c with acceptable level of stress. Both film resistivity and T_c have only a moderate dependence on film thickness. However since T_c determines the frequency cut-off of a micro-wave strip-line, this data is important for device characterization. A similar picture was observed previously by Wang et al. for NbN films [16].

XRD analysis shows no considerable difference in the XRD patterns of 300 nm thick (Nb,Ti)N films deposited on Si, glass, or sapphire wafers, when compared with the changes in XRD patterns caused by a change in the sputtering pressure of 1 mTorr. This indicates that the heat conductivity of the wafer plays only a minor role in the film growth, compared to other technological parameters. All films deposited on Si, glass and, sapphire wafers show a more pronounced [200] peak for thinner films (Fig. 3). Similar observation of competitive growth of [111] and [100] oriented grains was reported by L. Hultman *et. al.* for the TiN films [17].

Cross-sectional TEM analysis of 150 nm thick (Nb,Ti)N film on sapphire wafer (Fig. 4) shows a rapid increase in the grain size with film thickness and a more pronounced columnar structure for the upper layers of the film. This data is in good correlation with the broadening of the XRD peaks for thin films. The flattening of the ratio of [111] and [200] XRD peak intensity curves for 250-300 nm thick films (Fig. 3) indicates that film growth reaches an equilibrium at this thickness, which is compatible with the thickness of the (Nb,Ti)N layers used in mixer production. These changes indicate that the film crystallinity improves with the film thickness. In other words, the growth mode has a tendency to change from the ZT to the Z2 structural zone as the thickness of the film increases [18]. This results in an increase in T_c and a reduction in film resistivity with film thickness, for films deposited on Si, glass, and sapphire substrates. We believe that misfit dislocations cause the T_c degradation with film thickness for the epitaxial films deposited on MgO wafers.

We have also examined the dependence of intrinsic stress on film thickness, since it shows a nonlinear behavior versus thickness,

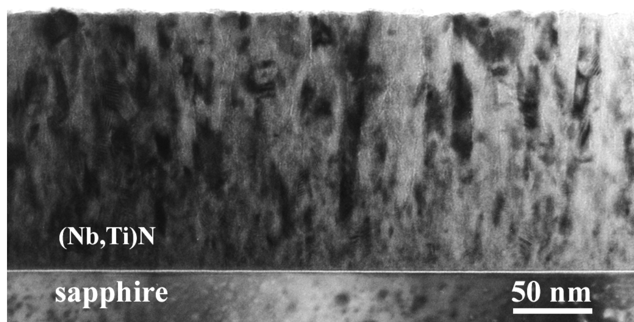

Fig. 4 Cross-sectional TEM view of (Nb,Ti)N film.

and this may cause a lattice distortion responsible for the T_c degradation. Fig. 5 illustrates the intrinsic stress and T_c dependencies on film thickness for (Nb,Ti)N films deposited at 6 and 9 mTorr. As we can see, the T_c degradation for thin films does not correlate with the stress curve for the almost stress-free film. Thus, we conclude that intrinsic stress does not cause the T_c degradation of thin films.

Because Θ-2Θ XRD scans reveal considerable fractions of the gains with [111] and [200] planes parallel to the substrate surface for non-epitaxial films and surface diffusion depends upon the crystallographic plane parallel to the substrate surface, we expect the film properties in-plane to be different. We have estimated the in-plane film homogeneity from ac susceptibility data. 300 nm thick epitaxial films deposited on MgO wafers show much better homogeneity when compared with films deposited on other wafers, since the transition width of epitaxial (Nb,Ti)N films is 0.1 K in this experiment, while films of the same thickness deposited on glass, Si, and sapphire wafers show transition widths of ≈ 0.3 K.

V. Conclusions

We have compared the properties of NbN, (Nb,Ti)N, and (Nb,Zr)N, deposited on glass and MgO wafers at ambient substrate temperature. The best properties are observed for (Nb,Ti)N films sputtered from a NbTi alloy target with 30 at. % Ti. (Nb,Ti)N films deposited on Si, sapphire, and glass wafers show a considerable degradation of T_c with film thickness due to poor crystallinity of the bottom layers of the films. Utilization of MgO wafers allows us to produce epitaxial (Nb,Ti)N films with improved properties and better homogeneity.

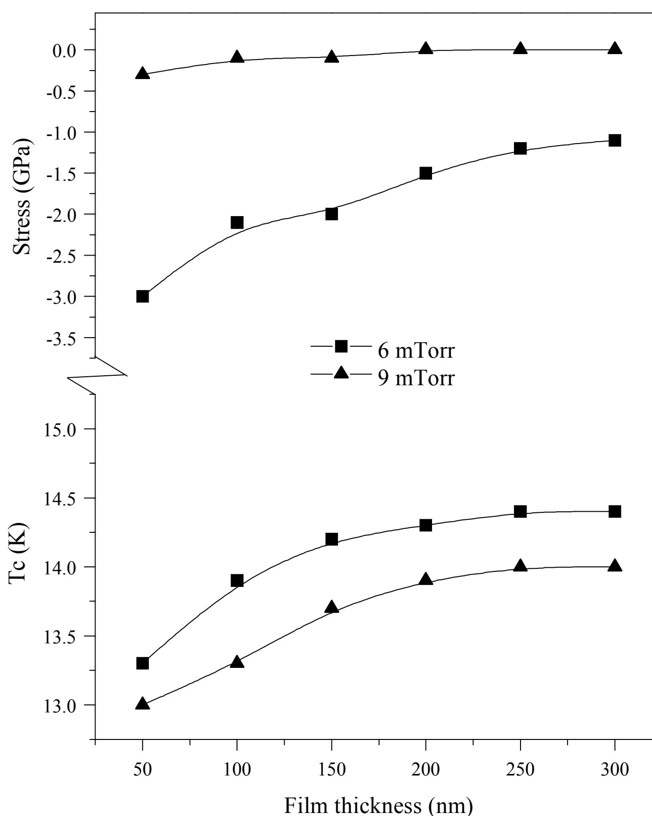

Fig. 5 T_c and film stress versus (Nb,Ti)N film thickness for the films sputtered under pressure of 6 and 9 mTorr on glass substrates.

References

[1] S. Kuriki, M. Matsuda, and A. Noya, "DC Squids made of NbN/a-Si/NbN tunnel junctions," *IEEE Trans. Magn.*, vol. 23, pp. 1064-1067, March 1987.

[2] M. Aoyagi, A. Shoji, S. Kosaka, H. Kakagawa, and S. Takada, "Submicron NbN Josephson tunnel junction for digital applications," *IEEE Trans. Magn.*, vol. 25, p. 1223-1226, March 1989.

[3] Y. Uzawa, Z. Wang, A. Kawakami, "Terahertz NbN/AlN/NbN mixers with Al/SiO/NbN microstrip tuning circuits," *Appl. Phys. Lett.*, vol. 73, pp. 680-682, March 1998.

[4] J. Kawamura, J Chen, D. Miller, J. Kooi, J. Zmuidzinas, B. Bumble, H. G. LeDuc, J. Stern, "Low-noise submillimeter-wave NbTiN superconducting tunnel junction mixers," *Appl. Phys. Lett.*, vol. 75, pp. 4013-4015 , December 1999.

[5] B. D. Jackson et al., submitted to *Appl. Phys. Lett.*

[6] N. N. Iosad, B. D. Jackson, T. M. Klapwijk, S. N. Polyakov, P. N. Dmitiev, J. R. Gao, "Optimization of rf- and dc-sputtered NbTiN films for integration with Nb-based SIS junction," *IEEE Trans. Appl. Supercond.*, vol. 9, pp. 1716-1719, June 1999.

[7] N. N. Iosad, B. D. Jackson, F. Ferro, J. R. Gao, S. N. Polyakov, P. N. Dmitriev, T. M. Klapwijk, "Source optimization for magnetron sputter-deposition of NbTiN tuning elements for SIS THz detectors," *Supercond. Sci. Technol.*, vol. 12, pp. 736-740, November 1999.

[8] K. L. Westra, M. J. Brett and J. F. Vaneldik, "Properties of reactively sputtered NbN films," *J. Vac. Sci. Technol.*, vol. A8, pp. 1288-1292, May/June 1990.

[9] D. L. Smith, *Thin-Film Deposition: Principles and Practice.* New York: McGraw-Hill, Inc., 1995, pp. 186-192.

[10] J. Hlavac, *The Technology of Glass and Ceramics.* Amsterdam: Elsevier Scientific, 1983, pp. 177-178.

[11] E. V. Pechen, A. V. Varlashkin, S. I. Krasnosvobodtsev, B. Brunner, and K. F. Renk, "Pulsed-laser deposition of smooth high-Tc superconducting films using a synchronous velocity filter," *Appl. Phys. Lett.*, vol. 66, pp. 2292-2294, April 1995.

[12] L. E. Toth, *Transition Metal Carbides and Nitrides.* New York: Academic Press, 1971, pp. 230-231. .

[13] J. A. Thornton, "Influence of apparatus geometry and deposition conditions on the structure and topography of thick sputtered coatings", *J. Vac. Sci. Technol.*, vol. 11, pp. 666-670, July/August 1974.

[14] D. L. Smith, *Thin-Film Deposition: Principles and Practice.* New York: McGraw-Hill, Inc., 1995, pp. 159-161.

[15] S. N. Polyakov, A. T. Rakhimov, N. V. Suetin, M. A. Timofeev, A. A. Pilevskii, "Growth and structure of epitaxial diamond films grown on Si(111) single crystals," *JETP Lett.*, vol *65,* pp. 434-438, March 1997.

[16] Z. Wang, A. Kawakami, Y. Uzawa, B. Komiyama, "Superconducting properties and crystal structures of single-crystal niobium nitride thin films deposited at ambient substrate temperature," *J. Appl. Phys.*, vol. 79, pp. 7837-7842, May 1996.

[17] L. Hultman, J.–E. Sundgren, J. E. Greene, D. B. Dergstrom, I. Petrov, "High-flux low-energy (≈ 20 eV) N^+_2 ion irradiation during TiN deposition by reactive magnetron sputtering: Effects on microstructure preferred orientation," *J. Appl. Phys.*, vol. 78, pp. 5395-5403, November 1995.

[18] D. L. Smith, *Film Deposition: Principles and Practice.* New York: McGraw-Hill, Inc., 1995, pp. 159-161.